Available online at www.sciencedirect.com
ScienceDirect
Journal of Sound and Vibration 315 (2008) 100–117
JOURNAL OF SOUND AND VIBRATION
www.elsevier.com/locate/jsvi

Dynamic stability of a semi-circular pipe conveying harmonically oscillating fluid

Duhan Jung[a,1], Jintai Chung[b,*], Andre Mazzoleni[c]

[a]Department of Precision Mechanical Engineering, Graduate School, Hanyang University, 17 Haengdang-dong, Seongdong-gu, Seoul 133-791, Republic of Korea
[b]Department of Mechanical Engineering, Hanyang University, 1271 Sa-1-dong, Ansan, Kyunggi-do 425-791, Republic of Korea
[c]Department of Mechanical & Aerospace Engineering, North Carolina State University, 2601 Stinson Drive, Raleigh, NC 27695, USA

Received 13 December 2006; received in revised form 28 January 2008; accepted 30 January 2008
Handling Editor L.G. Tham
Available online 18 March 2008

Abstract

The dynamic stability of a semi-circular pipe conveying harmonically oscillating fluid is investigated in this study. For analysis, harmonically oscillating flow is regarded as a parametrically excited system with time-varying coefficients. Considering the extensibility and nonlinearity of the semi-circular pipe, the equations of motion and the associated boundary conditions are obtained by using the extended Hamilton principle. Applying Floquet theory to the derived equations, the stability of the pipe is analyzed for variations of the amplitude and oscillating frequency of the fluid velocity. The effects of the mean value for the fluid velocity on the stability are also analyzed. It is found that the semi-circular pipe may become unstable when the fluctuation frequency approaches some multiples or sum of the out-of-plane natural frequencies. Furthermore, it is observed that the instability regions increase with the mean value of the velocity. The results obtained via the stability analysis are verified by time responses computed by using a direct time integration method.

1. Introduction

The dynamic analysis of pipes conveying fluid is of considerable interest in engineering, because these pipes are widely used in various applications, e.g., refrigerators, air-conditioners, heat-exchangers, chemical plants, hydropower systems, etc. For this reason, pipe dynamics has been investigated by many researchers over the past 50 years. Even though most piping systems are composed of both straight and curved pipes, studies of curved pipes are much less numerous than those of straight pipes.

An early analytical model of a curved pipe conveying fluid was suggested by Chen [1,2]. Under the assumption that the centerline of the curved pipe is inextensible, he claimed that the curved pipe shows instability similar to that of a straight pipe when the fluid velocity exceeds a certain critical value. However, Hill and Davis [3] as well as Doll and Mote [4] found that a fluid-conveying curved pipe does not lose stability,

*Corresponding author. Tel.: +82 31 400 5287; fax: +82 31 406 5550.
E-mail address: jchung@hanyang.ac.kr (J. Chung).
[1]Currently with Samsung Electronics Co., Republic of Korea.

0022-460X/$ - see front matter © 2008 Elsevier Ltd. All rights reserved.
doi:10.1016/j.jsv.2008.01.062

even for a high fluid velocity, if the centerline is extensible. To resolve this contradiction, Misra et al. [5,6] analyzed two cases of fluid-conveying curved pipes with inextensible and extensible centerlines. They concluded that the curved pipe model with an extensible centerline is more reasonable than the curved pipe model with an inextensible centerline. After their studies were reported, the curved pipe model with an extensible centerline has been widely used by many researchers. For example, Dupuis and Rousselet [7,8] derived the nonlinear governing equations of curved pipes conveying fluid assuming an extensible centerline. In Refs. [5–8], the equations of motion were derived with the fluid velocity based on Love's kinematical relations [9]. Since this velocity expression is valid only for the inextensible theory, Jung et al. [10] presented a new expression for the fluid velocity for an extensible pipe and they derived the equations for a semi-circular pipe conveying fluid. Recently, in-plane and out-of-plane motions of a semi-circular pipe conveying fluid with constant velocity has been analyzed by Jung and Chung [11]. They discussed some modeling issues related to the nonlinearity of the circumferential strain and stress. They recommend a model using the Lagrange strain and a linearized stress to compute dynamic responses efficiently while still maintaining accuracy.

The dynamics of a pipe conveying harmonically oscillating flow has become an interesting research topic. The fluid velocity in pipes of refrigerators or air-conditioners oscillates with a harmonic pattern because pump pressure varies harmonically. Severe noise and vibration are often generated by harmonically oscillating flow in a pipe system. In spite of the interest by engineers in curved pipes with harmonically oscillating flows, only a few of studies on this topic have been performed. All of the studies mentioned above concern pipes conveying fluid with constant velocity. Related to pipes conveying an oscillating flow, some researchers studied only straight pipes, not curved pipes. Chen [12] examined the stability of a straight pipe conveying harmonically oscillating flow and he found the possibility of parametric instabilities. Similarly, Paidoussis et al. [13,14] dealt with the dynamic stability of straight pipes containing harmonically perturbed flow. On the other hand, Lee and Chung [15] investigated the dynamics of piping system with internal unsteady flow. To the authors' knowledge, the curved pipe with harmonically oscillating flow has not been analyzed yet.

The purpose of this study is to investigate the dynamic stability of a semi-circular pipe conveying harmonically oscillating fluid. Assuming that the centerline is extensible, the nonlinear governing equations for the semi-circular pipe are derived by using the extended Hamilton principle. In the equations, the fluid velocity is regarded as a sinusoidal function with a non-zero mean value. Applying Floquet theory to the equations of motion, the parametric instabilities due to harmonically oscillating fluid are investigated. Furthermore, in order to verify the validity of the stability analysis, the dynamic time responses of the pipe are computed by using the generalized-α time integration method [16].

2. Modeling

Consider a semi-circular pipe conveying fluid, shown in Fig. 1, which is clamped at both ends. The semi-circular pipe has centerline radius R, the pipe mass density ρ_p and the fluid mass density ρ_f. The outer diameter and thickness of the pipe cross section are represented by d_o and h, respectively. The XYZ coordinate system is a space fixed inertial frame while the xyz coordinate system is a local coordinate system fixed at the centerline of the un-deformed pipe. The orientations of these two coordinates are defined by the angle θ measured from the X-axis. The Z and z axes are perpendicular to the XY and xy planes and their directions follow the

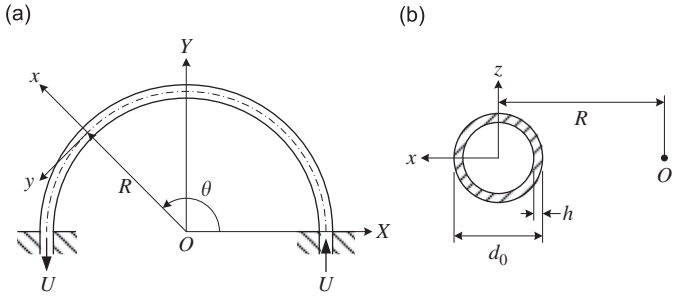

Fig. 1. Curved pipe conveying fluid with fluid velocity $U(t)$: (a) top view; and (b) cross section.

right-hand rule. The fluid conveyed by the pipe is assumed to be inviscid and incompressible and the flow in the pipe is treated as an irrotational plug flow. Since the fluid velocity profile in the pipe is spatially uniform, the fluid velocity $U(t)$ can be represented by a prescribed function that varies harmonically with time.

In this study, the semi-circular pipe is modeled as an extensible Euler-Bernoulli beam. Since the pipe diameter is small compared to both the centerline radius and the overall pipe length, the effects of the rotary inertia and shear deformation are negligible. Therefore, the cross section perpendicular to the central axis or the y-axis remains perpendicular to the central axis even after deformation. It is also assumed that the torsion-induced warping of the cross section is negligibly small. According to the Euler–Bernoulli beam theory, the displacements of a point on the pipe in the x, y, and z directions can be expressed as

$$u_x = u(\theta,t) + z\phi(\theta,t), \quad u_y = v(\theta,t) + x\phi_i(\theta,t) - z\phi_o(\theta,t), \quad u_z = w(\theta,t) - x\phi(\theta,t), \tag{1}$$

where u, v and w, are the radial (x-directional), circumferential (y-directional) and transverse (z-directional or out-of-plane) displacements of an arbitrary point on the centerline, respectively; ϕ is the twisting angle due to torsion about the y-axis; ϕ_I is the rotation angle about the z-axis due to the in-plane bending deformation; and ϕ_o is the rotation angle about the x-axis due to the out-of-plane bending deformation. It can be found from Ref. [17] that the rotation angles ϕ_I and ϕ_o are given by

$$\phi_i(\theta,t) = -(u' - v)/R, \quad \phi_o(\theta,t) = w'/R, \tag{2}$$

where the prime $()'$ stands for the partial derivative with respect to θ.

The geometrical nonlinearity considered in this study is due to the large deflection of the semi-circular pipe. When the flexural pipe undergoes vibration, the displacements of the pipe are often large. For large pipe deflections, the strains can be described by Lagrange strain theory which provides the nonlinear strain–displacement relations. Using the Lagrange theory, the circumferential normal strain of a point on the centerline can be written as

$$\varepsilon_y^c = \bar{\varepsilon}_y + \tfrac{1}{2}(\bar{\varepsilon}_y)^2 + \tfrac{1}{2}(\phi_i)^2 + \tfrac{1}{2}(\phi_o)^2, \tag{3}$$

where $\bar{\varepsilon}_y$ is a linearized strain given by

$$\bar{\varepsilon}_y = (u + v')/R. \tag{4}$$

Note that the first term on the right-hand side of Eq. (3) is linear but the other terms are nonlinear. Since the normal strain is related to both the in-plane and out-of-plane rotations, as shown in Eq. (3), the radial, circumferential and transverse displacements are fully coupled to each other. On an arbitrary point in the pipe, the circumferential normal strain may be represented by

$$\varepsilon_y = \varepsilon_y^c + x\phi_i'/R - z(\phi_o' - \phi)/R. \tag{5}$$

Even though the circumferential strain is nonlinear, the other non-zero strains, i.e., the shear strains, can be treated as linear strains. The reason is because the nonlinearity in the shear strains is negligible under the assumption that the plane cross section remains plane after deformation. Therefore, the linear shear strains can be expressed as

$$\gamma_{xy} = z(\phi' + \phi_o)/R, \quad \gamma_{yz} = -x(\phi' + \phi_o)/R. \tag{6}$$

The stress–strain relations in the semi-circular pipe can be easily obtained by assuming that the material of the pipe is homogeneous, isotropic, elastic and Hookean. Moreover, if the pipe is slender, in other words, if d_0 is much smaller than R, not only the normal stresses σ_x and σ_z but the shear stress τ_{xz} can also be neglected. In this circumstance, the circumferential normal stress and two transverse shear stresses may be written as

$$\sigma_y = E\varepsilon_y, \quad \tau_{xy} = G\gamma_{xy}, \quad \tau_{yz} = G\gamma_{yx}, \tag{7}$$

where E and G are Young's modulus and the shear modulus of the pipe, respectively.

3. Equations of motion

The strain energy of the semi-circular pipe is a function of the strains and stresses. The variation of the strain energy for the pipe can be represented by

$$\delta V = \int_0^{\pi} \int_A (\sigma_y \delta\varepsilon_y + \tau_{xy}\delta\gamma_{xy} + \tau_{yz}\delta\gamma_{yz}) R \, \mathrm{d}A \, \mathrm{d}\theta, \tag{8}$$

where δ is the variation operator and A is the cross sectional area of the pipe. Introduction of Eq. (7) into Eq. (8), after some manipulations, yields

$$\delta V = \int_0^{\pi} [RQ\delta\bar{\varepsilon}_y^c + M_x\delta\phi_i' + M_z\delta(\phi_o' - \phi) + M_y\delta(\phi' + \phi_o)] \, \mathrm{d}\theta, \tag{9}$$

where Q is the circumferential resultant force, M_x is the resultant in-plane bending moment, M_y is the resultant twisting couple, and M_z is the resultant out-of-plane bending moment. These resultant force and moments may be expressed as

$$Q = EA\bar{\varepsilon}_y, \quad M_x = EI(w'' - R\phi)/R^2, \quad M_y = GJ(R\phi' + w')/R^2, \quad M_z = EI(v - u')/R^2 \tag{10}$$

in which I is the area moment of inertia about both the x and z axes and J is the polar area moment of inertia about the y-axis.

To obtain the kinetic energy of the fluid-conveying semi-circular pipe, both the pipe velocity and the fluid velocity need to be expressed in terms of displacements u, v, w, and ϕ. After the pipe is deformed, the displacement vector of a point in the pipe can be expressed as

$$\mathbf{r} = (R + x + u_x)\mathbf{e}_x + u_y\mathbf{e}_y + (z + u_z)\mathbf{e}_z, \tag{11}$$

where $\mathbf{e}_x$, $\mathbf{e}_y$, and $\mathbf{e}_z$ are unit vectors corresponding to the x, y and z directions, respectively. Differentiation of the displacement vector with respect to time, after substituting Eqs. (1) into Eq. (11), results in the following expression for pipe velocity:

$$\mathbf{v}_p = \bar{\mathbf{v}}_p + x(\dot{\phi}_i\mathbf{e}_y - \dot{\phi}\mathbf{e}_z) + z(\dot{\phi}\mathbf{e}_x - \dot{\phi}_o\mathbf{e}_y), \tag{12}$$

where the superposed dot represents the partial derivative with respect to time and $\bar{\mathbf{v}}_p$ is the velocity of a point on the pipe centerline given by

$$\bar{\mathbf{v}}_p = \dot{u}\mathbf{e}_x + \dot{v}\mathbf{e}_y + \dot{w}\mathbf{e}_z. \tag{13}$$

The material derivative of the displacement vector leads to a fluid velocity, which has been recently introduced in Ref. [10]. As pointed out in Introduction, this fluid velocity is different form the velocity derived from Love's kinematical relations. The velocity obtained from the material derivative can be expressed as

$$\mathbf{v}_f = \bar{\mathbf{v}}_f + x\boldsymbol{\psi}_z - z\boldsymbol{\psi}_x, \tag{14}$$

where $\bar{\mathbf{v}}_f$ is the fluid velocity in the centerline of pipe; $\boldsymbol{\psi}_x$ and $\boldsymbol{\psi}_z$ are the angular velocities of the fluid cross section about the x and z axes, respectively,

$$\bar{\mathbf{v}}_f = [\dot{u} + U(u' - v)/R]\mathbf{e}_x + [\dot{v} + U(R + u + v')/R]\mathbf{e}_y + [\dot{w} + Uw'/R]\mathbf{e}_z, \tag{15}$$

$$\boldsymbol{\psi}_x = -[\dot{\phi} + (U/R)(\phi' + \phi_o)]\mathbf{e}_x + [\dot{\phi}_o - (U/R)(\phi - \phi_o')]\mathbf{e}_y, \tag{16}$$

$$\boldsymbol{\psi}_z = -(U/R)\dot{\phi}_i\mathbf{e}_x + [\dot{\phi}_i + (U/R)(1 + \phi_i')]\mathbf{e}_y - [\dot{\phi} + (U/R)\phi']\mathbf{e}_z. \tag{17}$$

When the torsional vibration is considered, the kinetic energy of the fluid-conveying pipe can be expressed as

$$T = \frac{1}{2}\int_0^{\pi} (m_p\bar{\mathbf{v}}_p \cdot \bar{\mathbf{v}}_p + I_m\dot{\phi}^2 + m_f\bar{\mathbf{v}}_f \cdot \bar{\mathbf{v}}_f) R \, \mathrm{d}\theta, \tag{18}$$

where m_p, m_f and I_m are the pipe mass, fluid mass and polar mass moment of inertia per unit pipe length, respectively.

The equations of motion and the associated boundary conditions for the semi-circular pipe conveying fluid are derived by using the extended Hamilton principle [18]. For an open system with mass transport, the extended Hamilton principle can be written as

$$\int_{t_1}^{t_2} (\delta T - \delta V + \delta W_{\mathrm{nc}} - \delta M)\,\mathrm{d}t = 0, \tag{19}$$

where δW_{nc} is the virtual work done by the non-conservative forces and δM is the virtual momentum transport. The non-conservative forces do not exist during free vibration of the pipe, so the virtual work does not need to be considered. However, the momentum transport should be considered in deriving the equations of motion because the fluid can move across the pipe boundaries. For the given pipe system, the virtual momentum transport can be expressed as

$$\delta M = [m_f(\bar{\mathbf{v}}_f \cdot \delta\mathbf{r})(U\mathbf{e}_y \cdot \mathbf{n})]_0^{\pi}, \tag{20}$$

where $\mathbf{n}$ is an outward normal unit vector at the boundaries. Substituting Eqs. (9), (18) and (20) into Eq. (19), the coupled nonlinear equations of motion for the semi-circular pipe conveying fluid are obtained as follows:

$$\begin{aligned}(m_p + m_f)\ddot{u} + 2m_f U(\dot{u}' - \dot{v})/R + m_f U^2(u'' - u - 2v')/R^2 + m_f \dot{U}(u' - v)/R + EI(u^{iv} - v''')/R^4 \\ + (EA/R^2)(u + v') + (EA/R^3)(u^2 - uu'' - u'^2 + 3uv' + u'v - u'v'' - u''v' + vv'' + 2v'^2) = m_f U^2/R,\end{aligned} \tag{21}$$

$$\begin{aligned}(m_p + m_f)\ddot{v} + 2m_f U(\dot{u} + \dot{v}')/R + m_f U^2(2u' + v'' - v)/R^2 + m_f \dot{U}(u + v')/R + EI(u''' - v'')/R^4 \\ - (EA/R^2)(u' + v'') + (EA/R^3)(-3uu' + uv - 2uv'' - 3u'v' + vv' - 2v'v'') = -m_f \dot{U},\end{aligned} \tag{22}$$

$$\begin{aligned}(m_p + m_f)\ddot{w} + 2m_f U\dot{w}'/R + m_f U^2 w''/R^2 + m_f \dot{U}w'/R + EI(w^{iv} - R\phi'')/R^4 \\ - GJ(w'' + R\phi'')/R^4 - (EA/R^3)(uw'' + u'w' + v'w'' + v''w') = 0,\end{aligned} \tag{23}$$

$$I_m\ddot{\phi} - EI(w'' - R\phi)/R^3 - GJ(w'' + R\phi'')/R^3 = 0. \tag{24}$$

The associated boundary conditions are given by

$$u = u' = v = w = w' = \phi = 0 \quad \text{at} \quad \theta = 0, \pi. \tag{25}$$

Eqs. (21)–(24) predominantly represent the in-plane bending motion, the in-plane extensional motion, the out-of-plane bending motion and the torsional motion, respectively. Hence, it can be said that in-plane motion is governed by Eqs. (21) and (22) while the out-of-plane motions is governed by Eqs. (23) and (24). The equations of motion, given by Eqs. (21)–(24), are the same as those of Model 3 presented in Ref. [11] when $\dot{U} = 0$. Model 3 uses the Lagrange nonlinear strain and a linearized stress to derive the equations of motion. In addition, recall again that the fluid velocity expression obtained from the material derivative is used during the derivation.

In order to generalize the analysis results for the semi-circular pipe, it is desirable to transform the equations of motion into dimensionless equations. For this purpose, the following non-dimensional parameters are introduced:

$$\begin{aligned}&u^* = \frac{u}{L}, \quad v^* = \frac{v}{L}, \quad w^* = \frac{w}{L}, \quad t^* = \sqrt{\frac{EI}{(m_p + m_f)}}\frac{t}{L^2}, \quad \theta^* = \frac{R\theta}{L}, \quad U^* = \sqrt{\frac{m_f}{EI}}LU, \quad \omega_n^* = \sqrt{\frac{m_p + m_f}{EI}}L^2\omega_n, \\ &\mu = \frac{m_f}{m_p + m_f}, \quad a = \frac{AL^2}{I}, \quad b = \frac{GJ}{EI}, \quad c = \frac{(m_p + m_f)L^2}{I_m},\end{aligned} \tag{26}$$

where $L = \pi R$. Substitution of Eq. (26) into Eqs. (21)–(24) yields the following dimensionless equations of motion:

$$\begin{aligned}\ddot{u} + 2\sqrt{\mu}U(\dot{u}' - \pi\dot{v}) + U^2(u'' - \pi^2 u - 2\pi v') + \sqrt{\mu}\dot{U}(u' - \pi v) + u^{iv} - \pi v''' \\ + \pi a(\pi u + v') + a(\pi^3 u^2 - \pi uu'' - \pi u'^2 + 3\pi^2 uv' + \pi^2 u'v - u'v'' - u''v' + \pi vv'' + 2\pi v'^2) = \pi U^2,\end{aligned} \tag{27}$$

$$\ddot{v} + 2\sqrt{\mu}U(\pi\dot{u} + \dot{v}') + U^2(2\pi u' + v'' - \pi^2 v) + \sqrt{\mu}\dot{U}(\pi u + v') + \pi u''' - \pi^2 v'' - a(\pi u' + v'') + a(-3\pi^2 uu' + \pi^3 uv - 2\pi uv'' - 3\pi u'v' + \pi^2 vv' - 2v'v'') = -\sqrt{\mu}\dot{U}, \tag{28}$$

$$\ddot{w} + 2\sqrt{\mu}U\dot{w}' + U^2 w'' + \sqrt{\mu}\dot{U}w' + w^{iv} - \pi\phi'' - b(\pi^2 w'' + \pi\phi'') - a(\pi uw'' + \pi u'w' + v'w'' + v''w') = 0, \tag{29}$$

$$\ddot{\phi} - c(\pi w'' - \pi^2\phi) - bc(\pi w'' + \phi'') = 0. \tag{30}$$

In the above equations, the superscript asterisk (*) is deleted for simplicity of notations and the prime and dot represent differentiations with respect to θ^* and t^*, respectively. The corresponding dimensionless boundary conditions are given by

$$u = u' = v = w = w' = \phi = 0 \quad \text{at} \quad \theta = 0, 1. \tag{31}$$

In order to find approximate solutions in a finite-dimensional function space, the nonlinear equations of motion, given by Eqs. (27)–(30), are discretized with the assumption that the solutions are linear combinations of some basis functions. The radial, circumferential, out-of-plane and twist displacements can be expressed as

$$u(\theta, t) = \sum_{n=1}^{N} u_n(\theta)x_n^u(t), \quad v(\theta, t) = \sum_{n=1}^{N} v_n(\theta)x_n^v(t), \quad w(\theta, t) = \sum_{n=1}^{N} w_n(\theta)x_n^w(t), \quad \phi(\theta, t) = \sum_{n=1}^{N} \phi_n(\theta)x_n^\phi(t), \tag{32}$$

where N is the total number of the basis functions; $x_n^u(t)$, $x_n^v(t)$, $x_n^w(t)$ and $x_n^\phi(t)$ are functions of time to be determined; and $u_n(\theta)$, $v_n(\theta)$, $w_n(\theta)$ and $\phi_n(\theta)$ are the basis function or the comparison functions defined as follows:

$$u_n(\theta) = w_n(\theta) = \cosh\,\lambda_n\theta - \cos\,\lambda_n\theta - \frac{\cosh\,\lambda_n - \cos\,\lambda_n}{\sinh\,\lambda_n - \sin\,\lambda_n}(\sinh\,\lambda_n\theta - \sin\,\lambda_n\theta), \tag{33}$$

$$v_n(\theta) = \phi_n(\theta) = \sqrt{2}\,\sin\,n\pi\theta \tag{34}$$

in which λ_n satisfies

$$\cosh\,\lambda_n\,\cos\,\lambda_n - 1 = 0. \tag{35}$$

Eqs. (33) and (34) are well-known eigenfunctions for the bending and axial vibrations of a straight beam, respectively [19].

Discretized equations are obtained by applying the Galerkin method to Eqs. (27)–(30) with the series solutions of Eqs. (32). These discretized equations can be represented by a vector equation given by

$$\mathbf{M}\ddot{\mathbf{x}} + 2U\mathbf{G}\dot{\mathbf{x}} + [\mathbf{K} + U^2\mathbf{H} + \dot{U}\mathbf{G}]\mathbf{x} + \mathbf{N}(\mathbf{x}) = U^2\mathbf{f}_0 + \dot{U}\mathbf{f}_1, \tag{36}$$

where $\mathbf{M}$ is the mass matrix, $\mathbf{G}$ is the matrix related to the gyroscopic force, $\mathbf{K}$ is the structural stiffness matrix, $\mathbf{H}$ is the matrix related to the centrifugal force of fluid, $\mathbf{N}(\mathbf{x})$ is a nonlinear force vector, $\mathbf{P}_0$ and $\mathbf{P}_1$ are the external force vectors due to the fluid flow, and $\mathbf{x}$ is an unknown vector given by

$$\mathbf{x} = \{x_1^u, x_1^v, x_1^w, x_1^\phi, \ldots, x_N^u, x_N^v, x_N^w, x_N^\phi\}^{\mathrm{T}}. \tag{37}$$

The sizes of all the matrices are $4N \times 4N$ and the sizes of all the vectors are $4N \times 1$.

4. Stability analysis

A perturbation method is used in this study to obtain the steady-state equation and the perturbed equation for the semi-circular pipe conveying harmonically oscillating flow. When using this method, the displacement vector may be represented by the sum of a steady-state solution and small perturbation:

$$\mathbf{x}(t) = \mathbf{x}_0 + \Delta\mathbf{x}, \tag{38}$$

where $\mathbf{x}_0$ is the steady-state solution and $\Delta\mathbf{x}$ is the small perturbation. The harmonically oscillating fluid velocity can be expressed as

$$U = U_0(1 + \varepsilon\,\cos\,\Omega t), \tag{39}$$

where U_0 is the mean value of the fluid velocity, Ω is the fluctuation frequency of the fluid velocity, and ε is the amplitude of velocity fluctuation. It should be noted that the excitation parameter ε is a small quantity, because the velocity fluctuation is much smaller than the mean value. Substituting Eq. (38) into Eq. (36), the following matrix–vector equations are obtained:

$$[\mathbf{K} + U^2\mathbf{H} + \dot{U}\mathbf{G}]\mathbf{x}_0 + \mathbf{N}(\mathbf{x}_0) = U^2\mathbf{f}_0 + \dot{U}\mathbf{f}_1, \tag{40}$$

$$\mathbf{M}\,\Delta\ddot{\mathbf{x}} + 2U\mathbf{G}\,\Delta\dot{\mathbf{x}} + [\mathbf{K} + \mathbf{T}(\mathbf{x}_0) + U^2\mathbf{H} + \dot{U}\mathbf{G}]\,\Delta\mathbf{x} = 0, \tag{41}$$

where $\mathbf{T}(\mathbf{x}_0)$ is the tangential stiffness matrix given by

$$\mathbf{T}(\mathbf{x}_0) = \left.\frac{\partial N}{\partial x}\right|_{x=x_0}. \tag{42}$$

It should be noted that Eq. (40) is for the steady-state solution while Eq. (41) is for the small perturbation from the steady state.

Using the Floquet theory, the stability of the semi-circular pipe with harmonically oscillating flow is analyzed for variations of the oscillating frequency and amplitude of the velocity fluctuation. Eq. (41) may be rewritten as

$$\dot{\mathbf{y}} = \mathbf{F}\mathbf{y}, \tag{43}$$

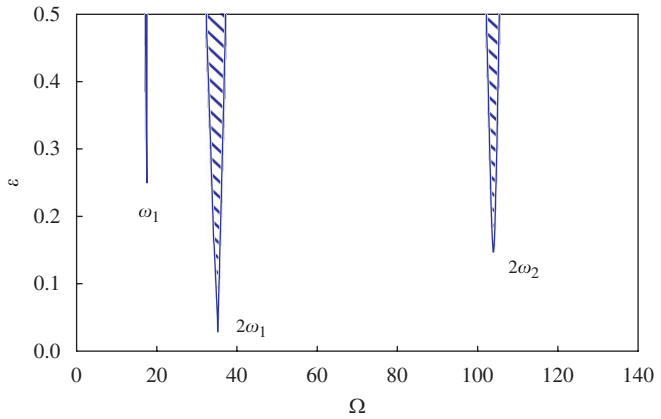

Fig. 2. Stability diagram for a curved pipe with harmonically oscillating flow when $U_0 = 2$.

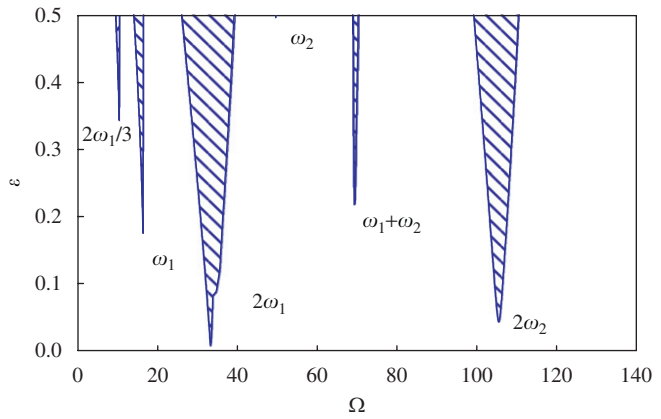

Fig. 3. Stability diagram for a curved pipe with harmonically oscillating flow when $U_0 = 4$.

where

$$\mathbf{y} = \begin{Bmatrix} \Delta\mathbf{x} \\ \Delta\dot{\mathbf{x}} \end{Bmatrix}, \quad \mathbf{F} = \begin{bmatrix} \mathbf{M} & \mathbf{0} \\ 2U\mathbf{G} & \mathbf{M} \end{bmatrix}^{-1} \begin{bmatrix} \mathbf{0} & \mathbf{M} \\ -\mathbf{K} - \mathbf{T}(\mathbf{x}_0) - U^2\mathbf{H} - \dot{U}\mathbf{G} & \mathbf{0} \end{bmatrix}. \tag{44}$$

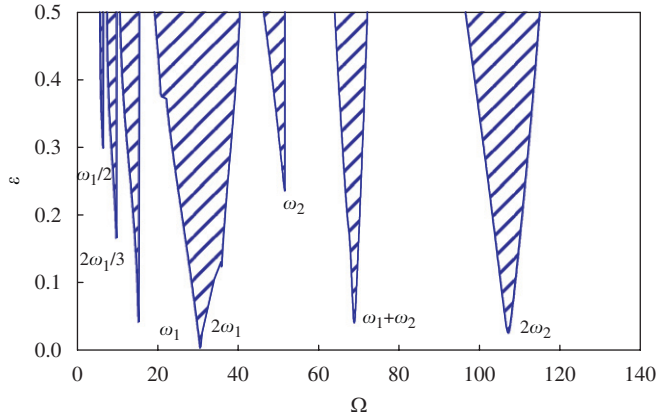

Fig. 4. Stability diagram for the curved pipe with harmonically oscillating flow when $U_0 = 6$.

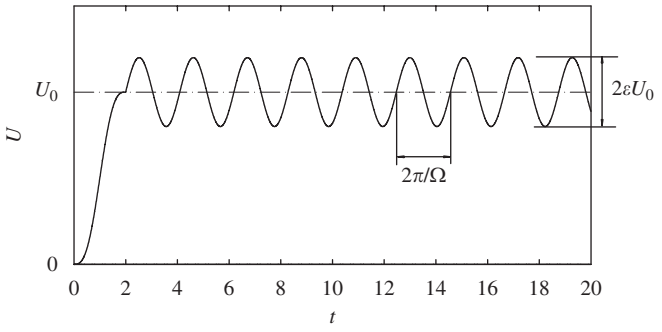

Fig. 5. Fluid velocity profile used in computation of the time responses.

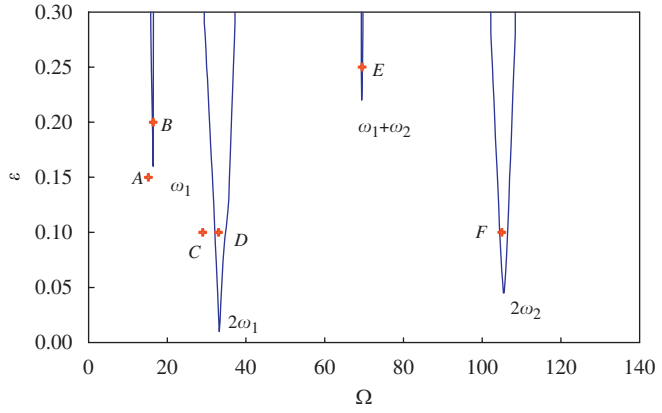

Fig. 6. Verification points in the stability diagram for the pipe with $U_0 = 4$.

Since **F** is a periodic function of time, the stability of the solution of Eq. (43) can be analyzed by the Floquet theory. Denoting the fundamental set of solutions by **U**, this fundamental matrix solution satisfies

$$\dot{\mathbf{U}} = \mathbf{F}\mathbf{U}. \tag{45}$$

Since $\mathbf{F}(t+T) = \mathbf{F}(t)$ where T is the period, $\mathbf{U}(t+T)$ is also a fundamental matrix solution, which is related to $\mathbf{U}(t)$ by

$$\mathbf{U}(t+T) = \mathbf{A}\mathbf{U}(t). \tag{46}$$

In general, the **A** matrix can be obtained by a direct time integration method. If the absolute values of all the eigenvalues of **A** are less than or equal to 1, the solution of Eq. (43) is stable. Otherwise, the solution becomes unstable.

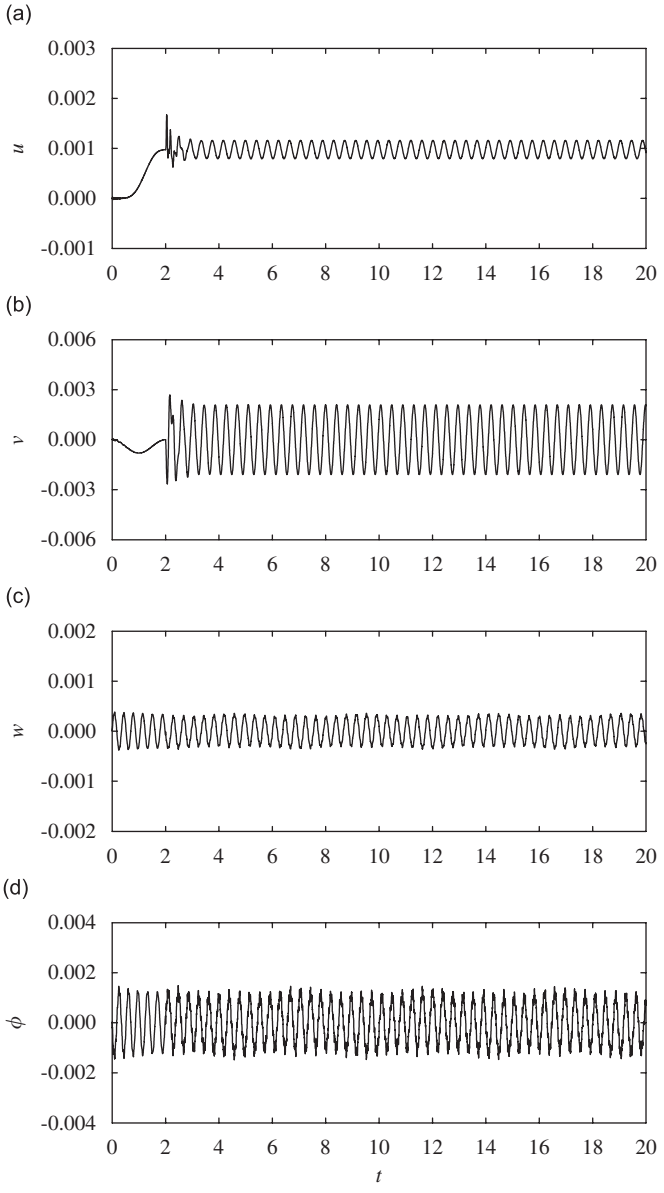

Fig. 7. Time responses of a curved pipe with $U_0 = 4$ when Ω and ε have values of the point A in Fig. 6: (a) the radial displacement, (b) the circumferential displacement, (c) the transverse displacement, and (d) the twist angle.

In the computations of this study, the following values are used: $\mu = 0.5$, $a = 10,000$, $b = 0.75$ and $c = 7000$. The parametric instability regions in the (Ω, ε)-space are shown in Figs. 2–4, where the hatched sections represent an unstable region and the unhatched sections represent a stable region. Figs. 2–4 show the instability regions when $U_0 = 2$, 4 and 6, respectively.

It can be seen from Figs. 2–4 that the instability is not related to the in-plane natural frequencies but is related instead to the out-of-plane natural frequencies. In these figures, ω_1 and ω_2 are the natural frequencies for the out-of-plane motion of the semi-circular pipe. As mentioned previously, the term out-of-plane motion refers to motion in the transverse or z-direction while the term in-plane-motion refers to motion in the xy-plane. From the fact that the natural frequencies for the in-plane motion do not appear in Figs. 2–4, it may be deduced that the unstable motion of the pipe is directly related to only the out-of-plane natural frequencies.

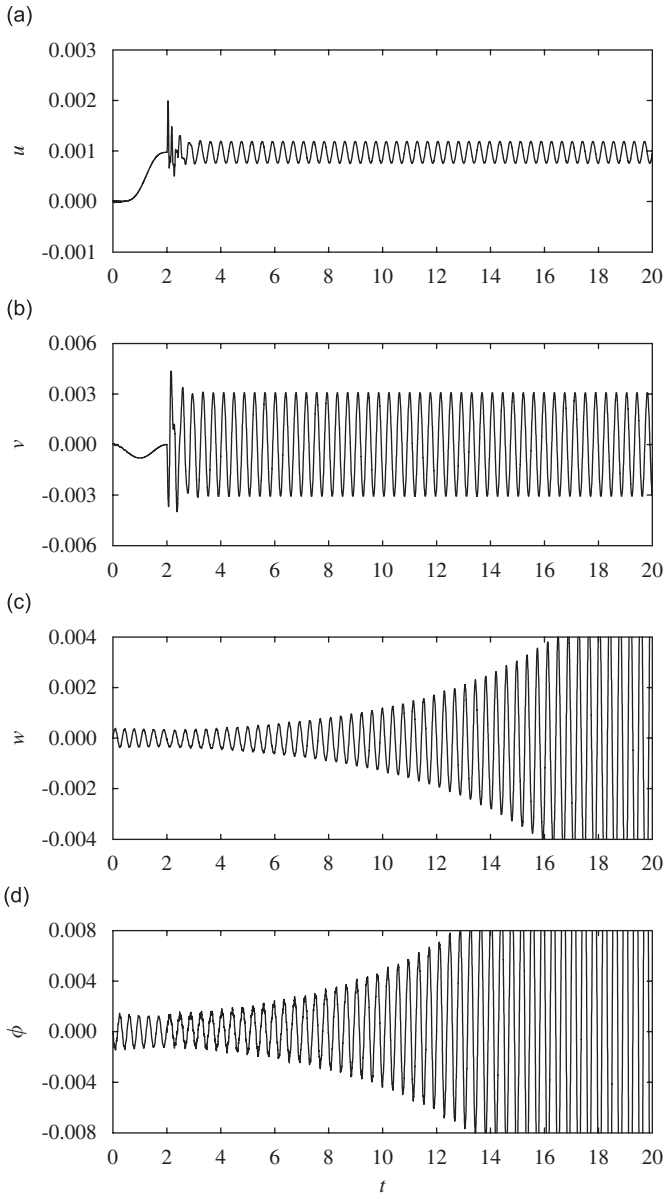

Fig. 8. Time responses of a curved pipe with $U_0 = 4$ when Ω and ε have values of the point B in Fig. 6: (a) the radial displacement, (b) the circumferential displacement, (c) the transverse displacement, and (d) the twist angle.

It is observed in Figs. 2–4 that motion of the semi-circular pipe may become unstable when the fluctuation frequency Ω approaches some multiples or sum of the out-of-plane natural frequencies. As shown in Fig. 2, the instability in motion of the pipe occurs at $\Omega \cong \omega_1$, $2\omega_1$ and $2\omega_2$ when the mean value of the fluid flow is given by $U_0 = 2$. Fig. 3 shows that the instability occurs at the fluctuation frequency corresponding to $\omega_1 + \omega_2$ in addition to ω_1, $2\omega_1$ and $2\omega_2$ if the mean value increases to $U_0 = 4$. It can be seen from Fig. 4 that the pipe with $U_0 = 6$ has one more fluctuation frequency of instability, $2/3\omega_1$, compared to the pipe with $U_0 = 4$. However, the motion of the pipe is not unstable when the fluctuation frequency is in the neighborhood of the second out-of-plane natural frequency, ω_2.

It is useful to investigate the influence of the mean value of the fluid flow on the instability in the motion of the semi-circular pipe. Figs. 2–4 show that the number of the fluctuation frequencies at which instability occurs increases with the mean value of the fluid flow. In addition, the instability regions grow in the

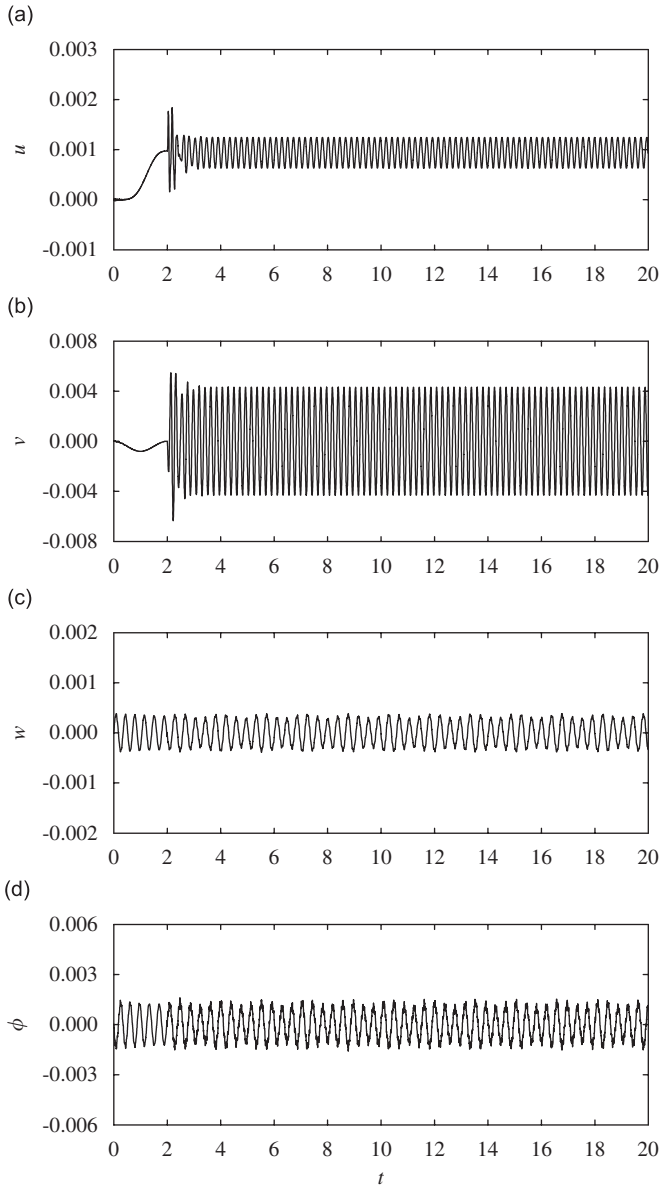

Fig. 9. Time responses of a curved pipe with $U_0 = 4$ when Ω and ε have values of the point C in Fig. 6: (a) the radial displacement, (b) the circumferential displacement, (c) the transverse displacement, and (d) the twist angle.

(Ω, ε)-space as the mean value of the flow increases. Finally, it is interesting that the amplitude of velocity fluctuation ε has an effect on the stability for the motion of the semi-circular pipe. If ε is very small, the pipe cannot be unstable for any values of U_0 and Ω. However, as ε becomes large, the instability tends to happen more easily. Furthermore, the range of Ω for which instability occurs increases with the value of ε.

The stability analysis for the semi-circular pipe with the harmonically oscillating flow is verified by investigating the time responses of the semi-circular pipe. These time responses are obtained by using the generalized-α time integration method [16], where the dimensionless time step size is chosen as 0.002 and the algorithmic parameters without numerical dissipation are adopted. Zero initial conditions of $\mathbf{x}(0) = \dot{\mathbf{x}}(0) = 0$ are imposed and a unit impulsive pressure is applied to the pipe. The time responses for the in-plane and

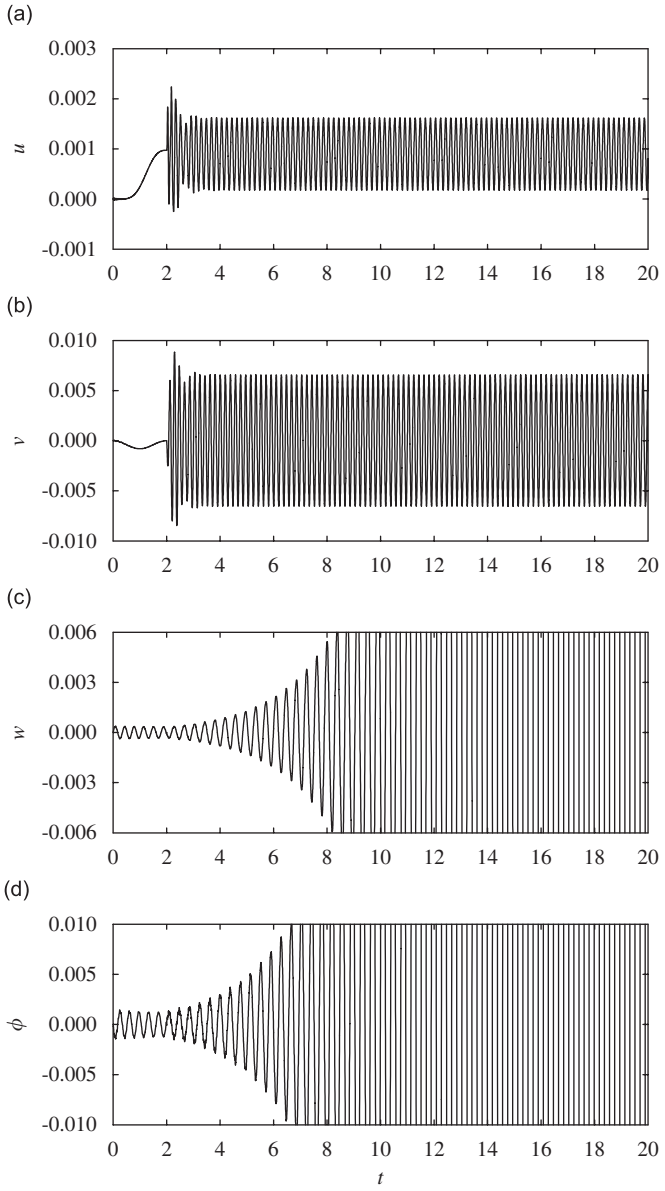

Fig. 10. Time responses of a curved pipe with $U_0 = 4$ when Ω and ε have values of the point D in Fig. 6: (a) the radial displacement, (b) the circumferential displacement, (c) the transverse displacement, and (d) the twist angle.

out-of-plane displacements are computed at the middle point on the pipe centerline. The harmonically oscillating fluid velocity is prescribed as

$$U(t) = \begin{cases} \dfrac{U_0(1+\varepsilon)}{2}\left(t - \dfrac{\sin \pi t}{\pi}\right) & \text{for } 0 \leqslant t \leqslant 2, \\ U_0[1 + \varepsilon \cos \Omega(t-2)] & \text{for } t \geqslant 2. \end{cases} \tag{47}$$

The velocity profile is presented in Fig. 5, which shows that the velocity smoothly increases from zero so as to avoid a sudden change in velocity from zero to the mean value. The time responses of the semi-circular pipe with harmonically oscillating flow are computed for the values of (Ω, ε) corresponding to six points (described

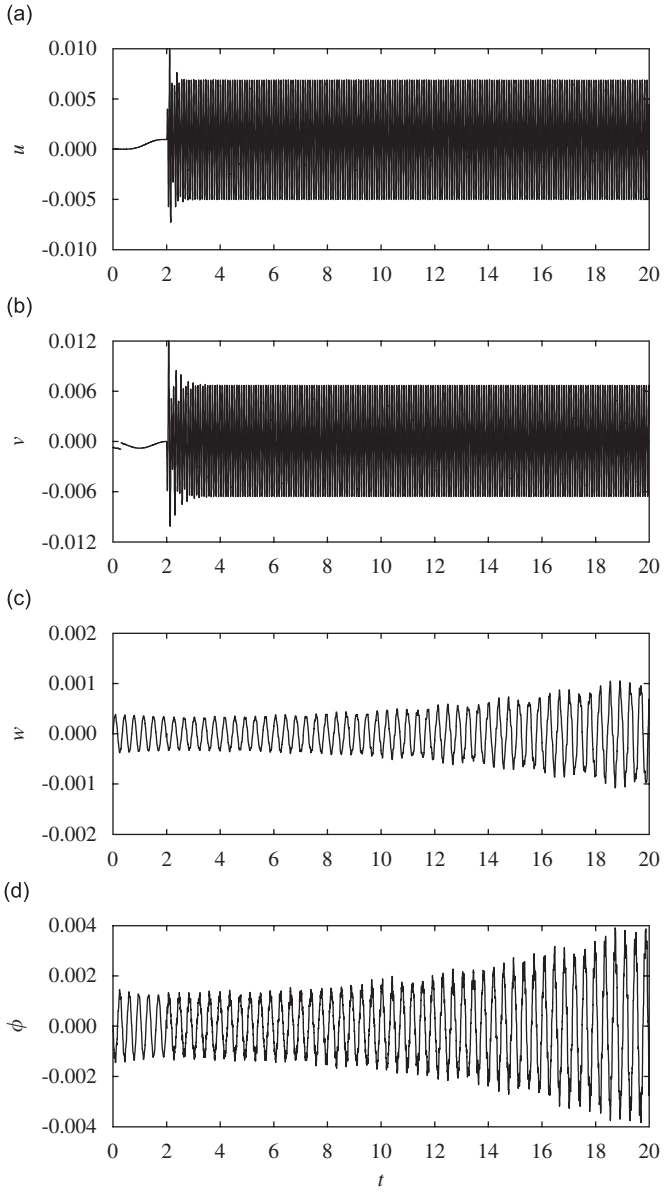

Fig. 11. Time responses of a curved pipe with $U_0 = 4$ when Ω and ε have values of the point E in Fig. 6: (a) the radial displacement, (b) the circumferential displacement, (c) the transverse displacement, and (d) the twist angle.

below) in Fig. 6, where the mean value of the fluid velocity is given by $U_0 = 4$. The values of (Ω, ε) for the six points are A (15.2, 0.15), B (16.4, 0.2), C (29.0, 0.1), D (33.0, 0.1), E (69.5, 0.25) and F (105.0, 0.1). Note that the points A and C are in the stable region while the points B, D, E and F are in the unstable region.

First, the time responses of the pipe with $U_0 = 4$ are investigated when Ω is in the neighborhood of ω_1. With the values of Ω and ε corresponding to the two points A and B of Fig. 6, the time responses of the radial, circumferential and transverse displacements and the twist angle are presented in Figs. 7 and 8, respectively. As shown in Fig. 7, when Ω and ε have the values of the point A, all the displacements and the twist angle are bounded. This means that the semi-circular pipe with small velocity fluctuation can be stable even though the fluctuation frequency coincides with the first out-of-plane natural frequency. However, Fig. 8 depicts that the transverse displacement w and the twist angle ϕ diverge as time increases when the values of Ω and ε correspond to the point B. These two figures verify the stability analysis around $\Omega = \omega_1$ of Fig. 6, in which the

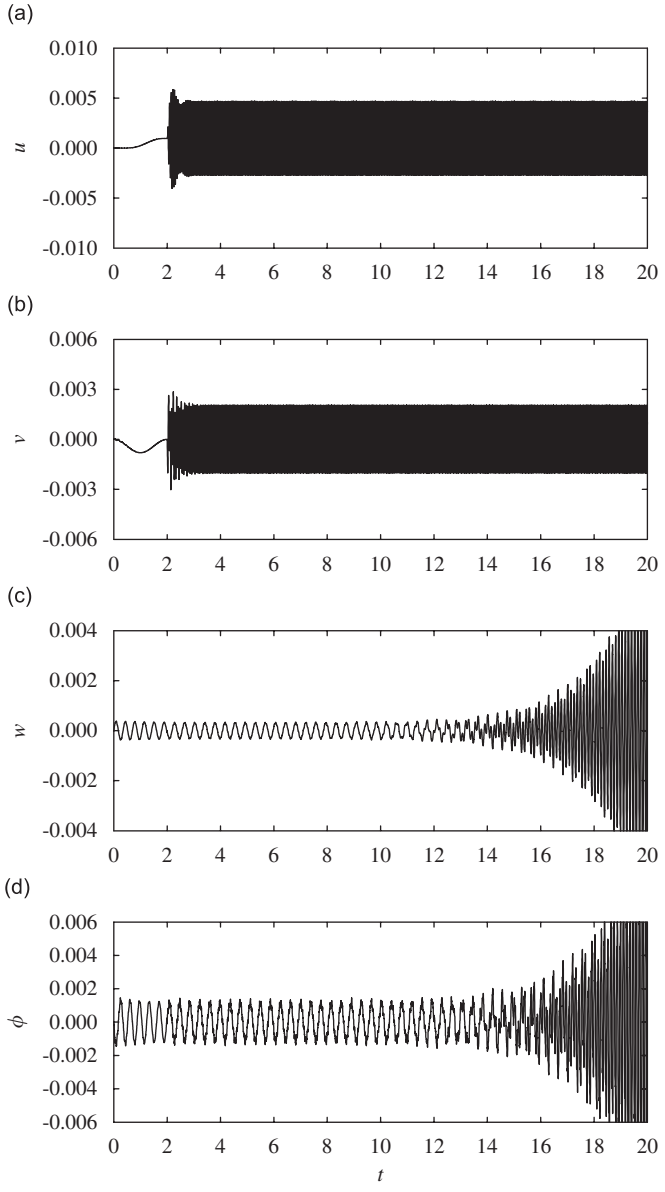

Fig. 12. Time responses of a curved pipe with $U_0 = 4$ when Ω and ε have values of the point F in Fig. 6: (a) the radial displacement, (b) the circumferential displacement, (c) the transverse displacement, and (d) the twist angle.

point A is in the stable region but the point B is in the unstable region. It is also shown in Fig. 8 that the in-plane displacements u and v do not diverge with time even if the values of Ω and ε are in the unstable region.

Similarly, the stability analysis results around $\Omega = 2\omega_1$ are examined with the time responses of the pipe. Figs. 9 and 10 show the time responses of the pipe when Ω and ε have the values of the points C and D, respectively. As predicted by the stability analysis, the time responses of all the displacements are bounded for the point C while the response of the transverse displacement and the twist angle are unbounded for the point D.

Next, the stability of the pipe is checked by the time responses when Ω is around $(\omega_1 + \omega_2)/2$ or $2\omega_2$. For verification, the responses of the pipe are investigated for the two points E and F of Fig. 6. These two points are in the unstable region. Figs. 11 and 12 demonstrate the time responses of the displacements for the values

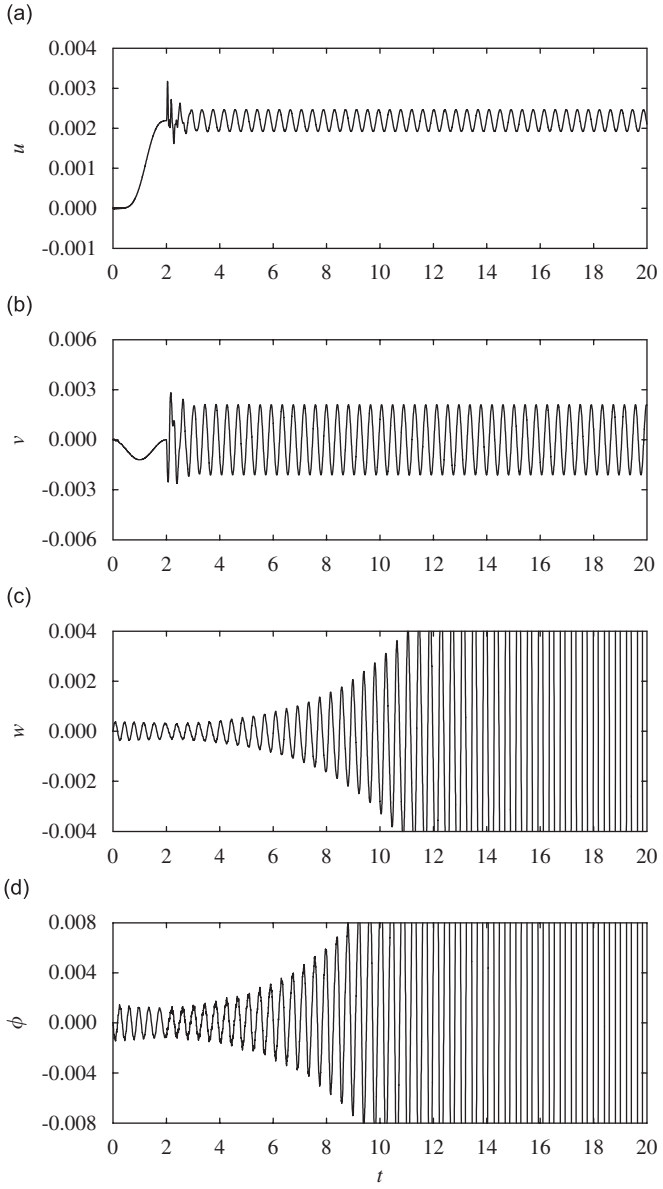

Fig. 13. Time responses of a curved pipe with $U_0 = 6$ when Ω and ε have values of the point A in Fig. 6: (a) the radial displacement, (b) the circumferential displacement, (c) the transverse displacement, and (d) the twist angle.

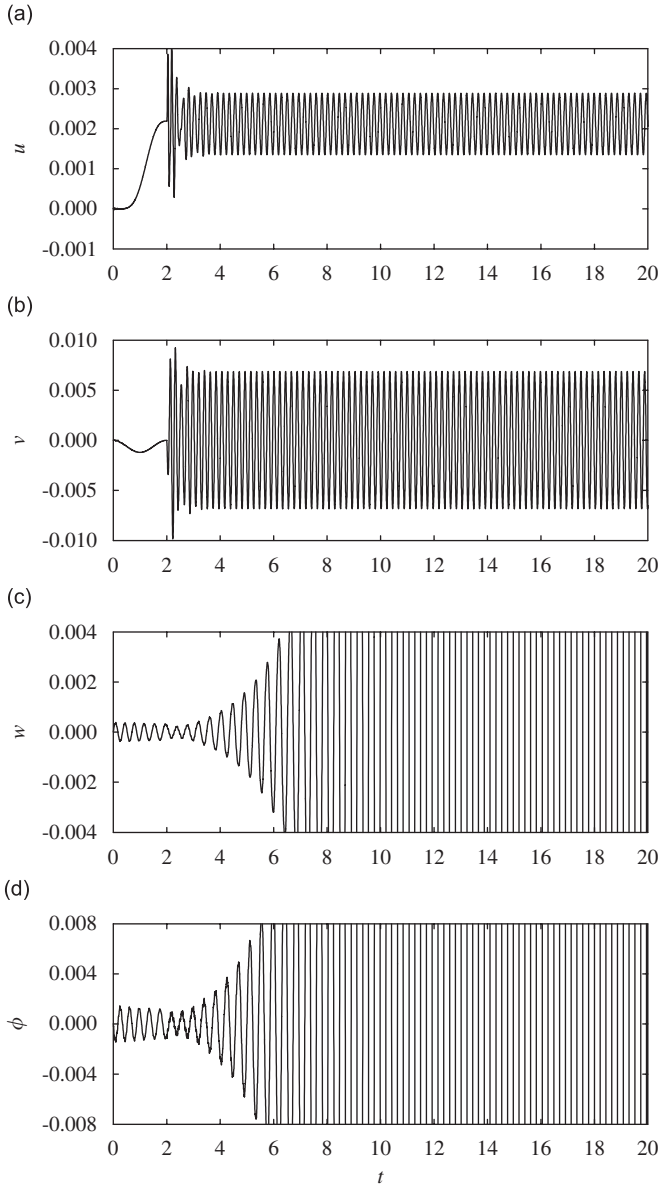

Fig. 14. Time responses of a curved pipe with $U_0 = 6$ when Ω and ε have values of the point C in Fig. 6: (a) the radial displacement, (b) the circumferential displacement, (c) the transverse displacement, and (d) the twist angle.

of Ω and ε corresponding to the points E and F, respectively. From these figures, it can be seen that the transverse displacement and the twist angle of the pipe are unbounded if time increases. In other words, similar instability shown in Figs. 8 and 10 occurs in Figs. 11 and 12.

Finally, it is interesting to observe the time response of the pipe with $U_0 = 6$ when Ω and ε possess the values for the points A and C in Fig. 6. These two points are in the stable region when $U_0 = 4$, as shown in Fig. 6; however, they come into the unstable region if U_0 increases to 6. This fact can be confirmed in Fig. 4 which shows the stability region for $U_0 = 6$. The time responses corresponding to the points A and C when $U_0 = 6$ are illustrated in Figs. 13 and 14. As predicted by Fig. 4, the transverse displacement and the twist angle diverge with time. Therefore, it can be seen that the behaviors of the time responses are in agreement with the stability results.

5. Conclusions

The dynamic stability of the motion of a semi-circular pipe is analyzed when the pipe conveys harmonically oscillating fluid. In this study, the semi-circular pipe is modeled as an extensible Euler–Bernoulli beam with a geometrical nonlinearity. Based on this model, four equations of motion are derived, which describe the radial, circumferential and transverse displacements and the twisting angle. These equations are discretized by applying the Galerkin method. A stability analysis is performed by using Floquet theory after applying a perturbation method. The results of the stability analysis are verified by time responses computed at several points on the stability diagram.

The results of the stability analysis can be summarized as follows:

(1) The out-of-plane natural frequencies of the pipe have an influence on the stability while the in-plane natural frequencies do not.
(2) The semi-circular pipe may become unstable when the fluctuation frequency Ω approaches some multiples or sum of the out-of-plane natural frequencies, for instance, in addition to ω_1, $2\omega_1$, $2\omega_2$, $2/3\omega_1$ and $\omega_1 + \omega_2$.
(3) The pipe is stable even when the fluctuation frequency is equal to the second out-of-plane natural frequency, ω_2.
(4) The number of fluctuation frequencies for which instability occurs increases with the mean value of the fluid velocity.
(5) The instability regions grow in the stability diagram as the mean value of the velocity of flow increases.
(6) For very small values of ε, the pipe may be stable regardless of the values of U_0 and Ω.
(7) The range of Ω in which instability occurs has a tendency to increase with the value of ε.

Acknowledgments

This work was supported by the research fund of Hanyang University (HY-2005-I). This support is gratefully acknowledged. The authors also gratefully acknowledge the support of the Mechanical and Aerospace Engineering Department at North Carolina State University.

References

[1] S.S. Chen, Vibration and stability of a uniformly curved tube conveying fluid, *Journal of Acoustical Society of America* 51 (1972) 223–232.
[2] S.S. Chen, Out-of-plane vibration and stability of curved tubes conveying fluid, *Journal of Applied Mechanics* 40 (1973) 362–368.
[3] J.L. Hill, C.G. Davis, The effect of initial forces on the hydrostatic vibration and stability of planar curved tube, *Journal of Applied Mechanics* 41 (1974) 355–359.
[4] R.W. Doll, C.D. Mote Jr., On the dynamic analysis of curved and twisted cylinders transporting fluids, *American Society of Mechanical Engineers Journal of Pressure Vessel Technology* 98 (1976) 143–150.
[5] A.K. Misra, M.P. Païdoussis, K.S. Van, On the dynamics of curved pipes transporting fluid. Part I: inextensible theory, *Journal of Fluids and Structures* 2 (1988) 221–244.
[6] A.K. Misra, M.P. Païdoussis, K.S. Van, On the dynamics of curved pipes transporting fluid. Part II: extensible theory, *Journal of Fluids and Structures* 2 (1988) 245–261.
[7] C. Dupuis, J. Rousselet, The equations of motion of curved pipes conveying fluid, *Journal of Sound and Vibration* 153 (1992) 473–489.
[8] C. Dupuis, J. Rousselet, Hamilton's principle and the governing equations of fluid-conveying curved pipes, *Journal of Sound and Vibration* 160 (1993) 172–174.
[9] A.E.H. Love, *A Treatise on the Mathematical Theory of Elasticity*, Dover, New York, 1944.
[10] D. Jung, J. Chung, H.H. Yoo, New fluid velocity expression in an extensible semi-circular pipe conveying fluid, *Journal of Sound and Vibration* 304 (2007) 382–390.
[11] D. Jung, J. Chung, In-plane and out-of-plane motions of an extensible semi-circular conveying fluid, *Journal of Sound and Vibration* 311 (2008) 408–420.
[12] S.S. Chen, Dynamic stability of a tube conveying fluid, *Journal of the Engineering Mechanics Division, Proceedings of the American Society of Civil Engineers* 97 (1971) 1469–1485.
[13] M.P. Païdoussis, N.T. Issid, Dynamic stability of pipes conveying fluid, *Journal of Sound and Vibration* 33 (1974) 267–294.

[14] M.P. Païdoussis, C. Sundararajan, Parametric and combination resonances of a pipe conveying pulsating fluid, *Journal of Applied Mechanics* 42 (1988) 780–784.
[15] S.I. Lee, J. Chung, New non-linear modelling for vibration analysis of a straight pipe conveying fluid, *Journal of Sound and Vibration* 254 (2002) 313–325.
[16] J. Chung, G.M. Hulbert, A time integration algorithm for structural dynamics with improved numerical dissipation: the generalized-α method, *Journal of Applied Mechanics* 60 (1993) 371–375.
[17] W. Kim, J. Chung, Free non-linear vibration of a rotating thin ring with the in-plane and out-of-plane motions, *Journal of Sound and Vibration* 258 (2002) 167–178.
[18] D.B. McIver, Hamilton's principle for systems of changing mass, *Journal of Engineering Mathematics* 7 (1972) 249–261.
[19] L. Meirovitch, *Analytical Methods in Vibrations*, Macmillan, New York, 1967.